Cell, Vol. 118, 579–590, September 3, 2004, Copyright ©2004 by Cell Press

Cytokinesis Monitoring during Development: Rapid Pole-to-Pole Shuttling of a Signaling Protein by Localized Kinase and Phosphatase in *Caulobacter*

Jean-Yves Matroule, Hubert Lam, Dylan T. Burnette, and Christine Jacobs-Wagner*
Department of Molecular, Cellular, and Developmental Biology
Yale University
P.O. Box 208103
New Haven, Connecticut 06520

Summary

For successful generation of different cell types by asymmetric cell division, cell differentiation should be initiated only after completion of division. Here, we describe a control mechanism by which *Caulobacter* couples the initiation of a developmental program to the completion of cytokinesis. Genetic evidence indicates that localization of the signaling protein DivK at the flagellated pole prevents premature initiation of development. Photobleaching and FRET experiments show that polar localization of DivK is dynamic with rapid pole-to-pole shuttling of diffusible DivK generated by the localized activities of PleC phosphatase and DivJ kinase at opposite poles. This shuttling is interrupted upon completion of cytokinesis by the segregation of PleC and DivJ to different daughter cells, resulting in disruption of DivK localization at the flagellated pole and subsequent initiation of development in the flagellated progeny. Thus, dynamic polar localization of a diffusible protein provides a control mechanism that monitors cytokinesis to regulate development.

Introduction

Asymmetric cell division is an important mechanism for the generation of cell diversity from bacteria to mammals. For correct cell fate specification by this mechanism, initiation of developmental programs relies on the segregation of cell fate determinants to only one daughter cell upon cell division. The temporal coupling between cell division and initiation of differentiation suggests that control mechanisms may exist.

The bacterium *Caulobacter crescentus* provides a simple experimental system to address this question because, in this organism, asymmetric cell division yields a daughter cell whose developmental fate is controlled by cell division (Ohta and Newton, 1996). At each cell cycle, *Caulobacter* divides asymmetrically to produce a stalked cell and a smaller swarmer cell, which subsequently differentiates into a stalked cell before initiating DNA replication (Figure 1). Genetic studies with mutations or drugs that inhibit cell division indicate that the developmental program of the swarmer progeny depends on the completion of previous cytokinesis (Huguenel and Newton, 1982; Terrana and Newton, 1976). This *swa*rmer *p*rogeny-specific (SwaPS) program includes the ordered sequence of flagellar rotation, pili synthesis, flagellum shedding, and ultimately stalk formation (Figure 1). It has been shown that the PleC and DivJ histidine kinases couple SwaPS development with cell division through the regulation of a shared single-domain response regulator, DivK (Ohta et al., 2000). Mutations in *pleC* block SwaPS development; thus, *pleC* mutants remain nonmotile, pililess, and stalkless after cell division (Sommer and Newton, 1989). Cold-sensitive mutants of *divJ* and *divK* were isolated as developmental suppressors of *pleC* mutants at 37°C and found to be filamentous at 24°C, indicating that DivJ and DivK are also involved in cell division (Sommer and Newton, 1991). The level of phosphorylated DivK (DivK-P) is reduced in a Δ*divJ* mutant, consistent with DivJ acting as a kinase of DivK (Wheeler and Shapiro, 1999). The biochemical function of PleC is less clear. In *pleC* mutants, the DivK-P level is increased relative to wild-type, suggesting that PleC directly or indirectly promotes DivK-P dephosphorylation (Wheeler and Shapiro, 1999).

DivJ, PleC, and DivK undergo spatial regulation. In predivisional cells, DivJ and PleC are asymmetrically localized with DivJ at the stalked pole and PleC at the flagellar pole (Wheeler and Shapiro, 1999). As shown in Figure 1, DivK is bipolarly localized during most of the predivisional stage but is released specifically from the flagellar pole right after completion of cytokinesis, when the cytoplasm is divided into two physically separated compartments (Jacobs et al., 2001). DivK localization is regulated by DivJ and PleC. In a kinase-inactive $divJ_{H338A}$ mutant, DivK localizes normally at the stalked pole, where $DivJ_{H338A}$ is located, but it fails to localize at the flagellar pole, indicating that the kinase activity of DivJ promotes localization of DivK at the flagellar pole (Lam et al., 2003). Conversely, PleC mediates the release of DivK from the flagellar pole because, in the absence of PleC catalytic function, DivK fails to delocalize from the flagellar pole at cell division (Lam et al., 2003). The role for the cell cycle-dependent polar localization of these signaling proteins has remained largely elusive, and the mechanism by which these proteins sense cytokinesis to control SwaPS development is unknown.

Here, we provide evidence that localized PleC phosphatase and DivJ kinase activities at opposite poles create a rapid shuttling of DivK between poles. This pole-to-pole shuttling provides a control mechanism that monitors cytokinesis to regulate initiation of SwaPS development.

Results and Discussion

DivK Localization at the Flagellar Pole Is Involved in Coupling SwaPS Development to Cytokinesis

As mentioned above, *pleC* mutants fail to release DivK from the flagellar pole (Figure 2A) and to initiate SwaPS development upon cell division, resulting in nonmotile,

*Correspondence: christine.jacobs-wagner@yale.edu

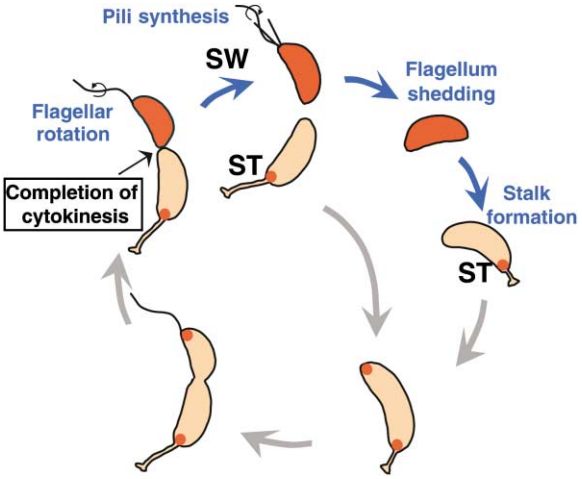

Figure 1. Completion of Cytokinesis Is Required for Initiation of a Developmental Sequence of Events in the Ensuing Cell Cycle of the Swarmer Progeny

The swarmer progeny-specific (SwaPS) developmental program (blue arrows) includes flagellar rotation, pili synthesis, flagellum shedding, and ultimately stalk formation. The cell cycle-dependent localization of DivK (red) culminates in the complete release of DivK from the flagellar pole upon completion of cytokinesis (division of the cytoplasm into two). SW, swarmer cell; ST, stalked cell.

pililess, and stalkless cells with paralyzed, unshed flagella. This suggested that a maintained localization of DivK at the flagellar pole after cytokinesis inhibited SwaPS development. To test this hypothesis, we examined the localization of a DivK mutant with a D90G mutation that suppresses all developmental defects of a *pleC*::Tn*5* mutant at 37°C (Sommer and Newton, 1991). $DivK_{D90G}$ fused to GFP was able to localize at the stalked pole of *pleC*::Tn*5* cells at 37°C but failed to significantly accumulate at the flagellar pole during the cell cycle (Figure 2A). A similar localization pattern was observed in a $pleC^+$ background (data not shown). The D90G mutation does not affect DivK phosphorylation (Hung and Shapiro, 2002). Therefore, it is the inability of $DivK_{D90G}$ to localize to the flagellar pole at 37°C that accounts for the suppression of *pleC* developmental defects. Thus, localization of DivK at the flagellar pole is involved in the inhibition of SwaPS development.

Next, we showed that DivK release from the flagellar pole was dependent on the completion of cytokinesis. Localization of wild-type DivK-GFP was followed after inhibition of cytokinesis using a strain (CJW933; Table 1) in which the essential cell division gene *ftsZ* was under the inducible xylose promoter. In the presence of xylose in the culture medium, the timing of DivK-GFP release from the flagellar pole occurred normally right after cytokinesis (Figure 2B). Removal of xylose resulted in FtsZ depletion and inhibition of cytokinesis, which in turn prevented the release of DivK-GFP from the flagellar pole; instead, DivK-GFP localization remained bipolar throughout cell elongation (Figure 2B).

In *Caulobacter*, cytokinesis in normal-sized cells produces a stalked daughter cell that is bigger than its swarmer cell sibling. Restoration of cytokinesis in elongated cells occurs at various locations, sometimes at a site closer to the stalked pole, to create stalked daughter cells smaller than their siblings (Figure 2C). Thus, to ascertain the identity of the poles, we used a strain (CJW979) in which DivK and DivJ (stalked pole marker) were fused to the monomeric forms of CFP and YFP (mCFP and mYFP), respectively. Restoration of cytokinesis by addition of xylose to elongated CJW979 cells resulted in delocalization of DivK-mCFP specifically from the pole distal to the stalked DivJ-mYFP pole; this was true even in the instances when cell division created a stalked progeny smaller than its sibling (Figure 2C), suggesting that DivK release is not sensitive to cell length. We made similar observations with cells treated with the β-lactam antibiotic cephalexin, which at sublethal concentration inhibits a later step of cell division (data not shown). Thus, DivK release from the flagellar pole is cytokinesis dependent.

If a control mechanism involving DivK localization at the flagellar pole specifies the known dependence of SwaPS development on cytokinesis, this dependence should be relieved by the D90G mutation in DivK, which prevents DivK from localizing to the flagellar pole. A relief of this dependence would permit SwaPS development to occur even when cytokinesis is inhibited, ultimately leading to the formation of a stalk at the pole where the flagellum was previously located. To test this hypothesis, cytokinesis was inhibited in synchronized wild-type *divK* (YB1585) and $divK_{D90G}$ (CJW1169) cells by FtsZ depletion. As previously described (Osley and Newton, 1977), inhibition of cytokinesis blocked SwaPS development in the wild-type *divK* background, yielding filaments with a stalk at one pole and a flagellum at the other (Figure 2D). In contrast, $divK_{D90G}$ cells initiated SwaPS development regardless of cytokinesis inhibition, yielding filamentous cells with a stalk at each pole (Figure 2D). This relief of dependence between cytokinesis and SwaPS development argues for the existence of a control mechanism.

Altogether, our data strongly suggest that the cytokinesis-dependent release of DivK from the flagellar pole is the molecular event that signals entry into SwaPS development in response to completion of cytokinesis.

The PleC Histidine Kinase Primarily Acts as a Phosphatase of DivK-P In Vivo

To unravel the mechanism by which the cell senses the completion of cytokinesis to release DivK from the flagellar pole, it was critical to understand how the asymmetrically localized DivJ and PleC histidine kinases control the localization of DivK at the flagellar pole. Previous studies have indicated that DivJ, through its kinase activity, mediates the localization of DivK at the flagellar pole by increasing the cellular concentration of DivK-P, suggesting that the flagellar pole has a higher affinity for the phosphorylated form of DivK (Lam et al., 2003). Consistently, nonphosphorylatable DivK mutants are unable to polarly localize (Lam et al., 2003). PleC, on the other hand, promotes DivK release from the flagellar pole by decreasing the concentration of DivK-P in the cell (Lam et al., 2003). While it has been proposed that PleC may indirectly affect DivK phosphorylation by inhibiting DivJ function (Wheeler and Shapiro, 1999), yeast two-hybrid experiments, together with genetic and bio-

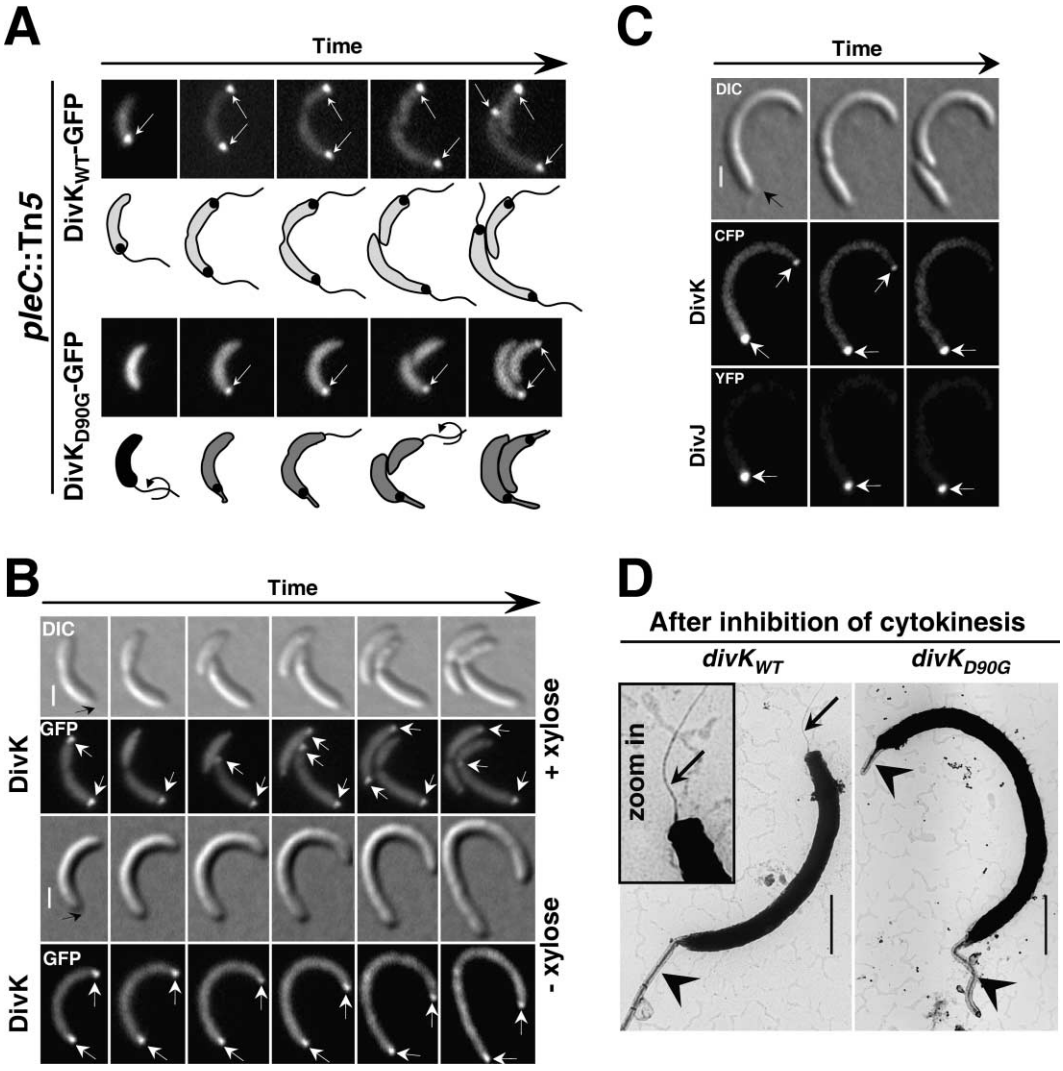

Figure 2. The Complete Release of DivK from the Flagellar Pole in Response to Cytokinesis Completion Allows Initiation of SwaPS Development

(A) DivK localization at the flagellar pole is involved in inhibition of SwaPS development. Time-lapse fluorescence microscopy was performed at 37°C with *pleC*::Tn*5* cells expressing either DivK-GFP or DivK$_{D90G}$-GFP. Arrows show polar signals.

(B) Inhibition of cytokinesis prevents DivK release from the flagellar pole. Time-lapse experiments with cells (CJW933) expressing DivK-GFP and in which *ftsZ* was under the control of the xylose inducible promoter. Cells were grown in the presence of 0.3% xylose, washed once, and spotted on an agarose-padded slide that contained medium either with xylose or without xylose to induce FtsZ depletion and inhibition of cell division. The black and white arrows indicate the stalk and polar localization of DivK-GFP, respectively. Scale bar, 1 μm.

(C) Restoration of cytokinesis in filamentous cells results in DivK release from the flagellar pole. After 1 hr of culture in the absence of xylose to induce FtsZ depletion and cell elongation, cytokinesis in elongated CJW979 cells expressing DivK-mCFP and DivJ-mYFP was restored by adding xylose (0.3%). The black and white arrows indicate the stalk and the polar signals, respectively.

(D) A *divK*$_{D90G}$ mutation relieves the dependence of SwaPS development on cytokinesis. After synchronization, FtsZ depletion and cell elongation were induced in wild-type *divK* (YB1585) and *divK*^{D90G} (CJW1169) cells by removal of xylose from the M5GG medium. Cells were visualized by transmission electron microscopy after negative staining with 1% uranyl acetate. Arrows and arrowheads show flagella and stalks, respectively. Scale bar, 1 μm.

chemical evidence, strongly argue in favor of a physical interaction between PleC and DivK (Hecht et al., 1995; Ohta and Newton, 2003; Sommer and Newton, 1991). Thus, PleC may directly stimulate DivK-P dephosphorylation. Such phosphatase activity has been described for other histidine kinases (Tomoromi et al., 2003).

Previous studies have demonstrated that the soluble PleC catalytic domain (PleC′) exhibits both DivK kinase and DivK-P phosphatase activities in vitro (Hecht et al., 1995; Wu et al., 1998). To determine which activity was dominant in vivo, we sought to uncouple PleC kinase and phosphatase activities and test the effects of this uncoupling on PleC functions in vivo. It has previously been shown that the balance of kinase and phosphatase activities of the *Escherichia coli* histidine kinase EnvZ can be altered by specific amino acid substitutions within the catalytic domain (Aiba et al., 1989; Hsing et al., 1998; Hsing and Silhavy, 1997). Based on an alignment between PleC and EnvZ, we made three independent substitutions in PleC residues (T614R, F778L, and H610A,

Table 1. Strains and Plasmids

Strains	Relevant Genotype or Description	
Caulobacter		
CJW27	CB15N (or NA1000) synchronizable variant strain of CB15	Evinger and Agabian, 1977
CJW332	CB15N *divJ*::*gent*	Wheeler and Shapiro, 1999
CJW366	CB15N/pMR20divK-gfp	Jacobs et al., 2001
CJW686	CB15N *pleC*::*pleC-myfp*	this study
CJW718	CB15N *pleC*::*pleC-myfp*/pMR20divK-mcfp	this study
CJW719	CB15N/pMR20divK-mcfp	this study
CJW788	CB15N Δ*pleC*/pJS14pleCT614R-myfp	this study
CJW801	CB15N *rec pleC*::*pleC-tdimer2 divJ-yfp*/pMR20divK-mcfp	this study
CJW858	CB15N *divJ*::*divJ-myfp*	this study
CJW864	CB15N Δ*pleC*/pJS14pleCH610A-yfp	this study
CJW865	CB15N *divJ*::*divJ-myfp*/pMR20divK-mcfp	this study
CJW878	CB15N Δ*pleC*/pJS14pleC-myfp	this study
CJW884	CB15N *divJ*::*gent*/pMR20divJ-myfpdivK-mcfp	this study
CJW885	CB15N Δ*pleC*/pJS14pleC-myfp/pMR20divK-mcfp	this study
CJW933	CB15N *ftsZ*::pBJM1/pMR20divK-gfp	this study
CJW942	CB15N *ftsZ*::pBJM1/pJS14pleC-myfp	this study
CJW977	CB15N *rec pleC-myfp divJ-tdimer2*/pMR20divK-mcfp	this study
CJW979	CB15N *ftsZ*::pBJM1/pMR20divJ-myfpdivK-mcfp	this study
CJW981	CB15N *ftsZ*::pBJM1/pJS14pleC-myfp/pMR20divK-mcfp	this study
CJW983	CB15N *divJ*::*gent*/pMR20divJ-myfp	this study
CJW984	CB15N *ftsZ*::pBJM1/pMR20divJ-myfp	this study
CJW1144	CB15N Δ*pleC*/pJS14pleCF778L-myfp	this study
CJW1162	CB15N *pleC*::Tn*5 xylX*::pBXdivK-gfp/pJS14pleCF778L	this study
CJW1164	CB15N *pleC*::Tn*5 xylX*::pBXdivK-gfp/pJS14pleCT614R	this study
CJW1167	CB15N *pleC*::Tn*5* Δ*divK xylX*::pBXdivK-gfp	this study
CJW1168	CB15N *pleC*::Tn*5* Δ*divK xylX*::pBXdivKD90G-gfp	this study
CJW1169	CB15N *divKD90G ftsZ*::pBJM1	this study
YB1585	CB15N *ftsZ*::pBJM1	Wang et al., 2001
E. coli		
S17-1	RP4-2, *Tc*::*Mu*, *KM*-Tn*7*, for plasmid mobilization	Simon et al., 1983
DH5α	cloning strain	Invitrogen
Plasmid	**relevant genotype or description**	**Reference or source**
pBluescriptKS (+)	AmpR cloning vector	Stratagene
pMR20	TetR low copy number broad host range vector	Roberts et al., 1996
pJS14	ChlR pBBR1-derived medium copy number broad host range vector	Jeffrey Skerker
pBGS18T	a derivative of pBGS18 (Spratt et al., 1986)	Alley, 2001
pBGent	GentR variant of pBGS18T	this study
pgfp	green fluorescent protein (GFP)	Clontech
pmyfp, pmcfp	monomeric variants of YFP and CFP	Zacharias et al., 2002
ptdimer2	tandem of two dimeric variants of DsRed (Dimer2)	Campbell et al., 2002
pMR20divK-egfp	pMR20 carrying *divK-gfp*	Jacobs et al., 2001
pMR20divK-mcfp	pMR20 carrying *divK-mcfp*	this study
pMR20divJ-myfp	pMR20 carrying *divJ-myfp*	this study
pMR20divJ-myfp,divK-mcfp	pMR20 carrying *divJ-myfp* and *divK-mcfp*	this study
pJS14pleC-myfp	pJS14 carrying *pleC-myfp*	this study
pJS14pleCH610A-yfp	pJS14 carrying *pleCH610-yfp*	Lam et al., 2003
pJS14pleCT614R-myfp	pJS14 carrying *pleCT614R-myfp*	this study
pJS14pleCF778L-myfp	pJS14 carrying *pleCF778L-myfp*	this study
pJS14pleCF778L	pJS14 carrying *pleCF778L*	this study
pJS14pleCT614R	pJS14 carrying *pleCT614R*	this study
pBGentpleC-myfp	pBGent carrying 5′ truncated *pleC-myfp*	this study
pBGentpleC-tdimer2	pBGent carrying 5′ truncated *pleC-tdimer2*	this study
pBXdivK-gfp	pBGent carrying *divK-gfp* and 800bp of *xylX* ORF	this study
pBXdivKD90G-gfp	pBGent carrying *divKD90G-gfp* and 800bp of *xylX* ORF	this study
pBJM1	pBGS18T carrying the N-term portion of *ftsZ*	Wang et al., 2001

H610 being the site of phosphorylation). The soluble catalytic domain of each mutant was purified and tested for its in vitro ability to autophosphorylate (autokinase activity), promote DivK phosphorylation (kinase activity), and dephosphorylate DivK-P (phosphatase activity). All three mutations resulted in abrogation both of autokinase and kinase activities of PleC compared to wild-type (Figure 3A). The phosphatase activity of each PleC′ mutant was assessed by incubating purified DivK-P with each PleC′ protein for various amounts of time (Figure 3B). The autophosphatase activity of DivK (Hecht et al., 1995), which is common among response regulators, was evaluated in reactions lacking PleC′ protein. Phosphatase activity was negligible for PleC′$_{T614R}$ and consid-

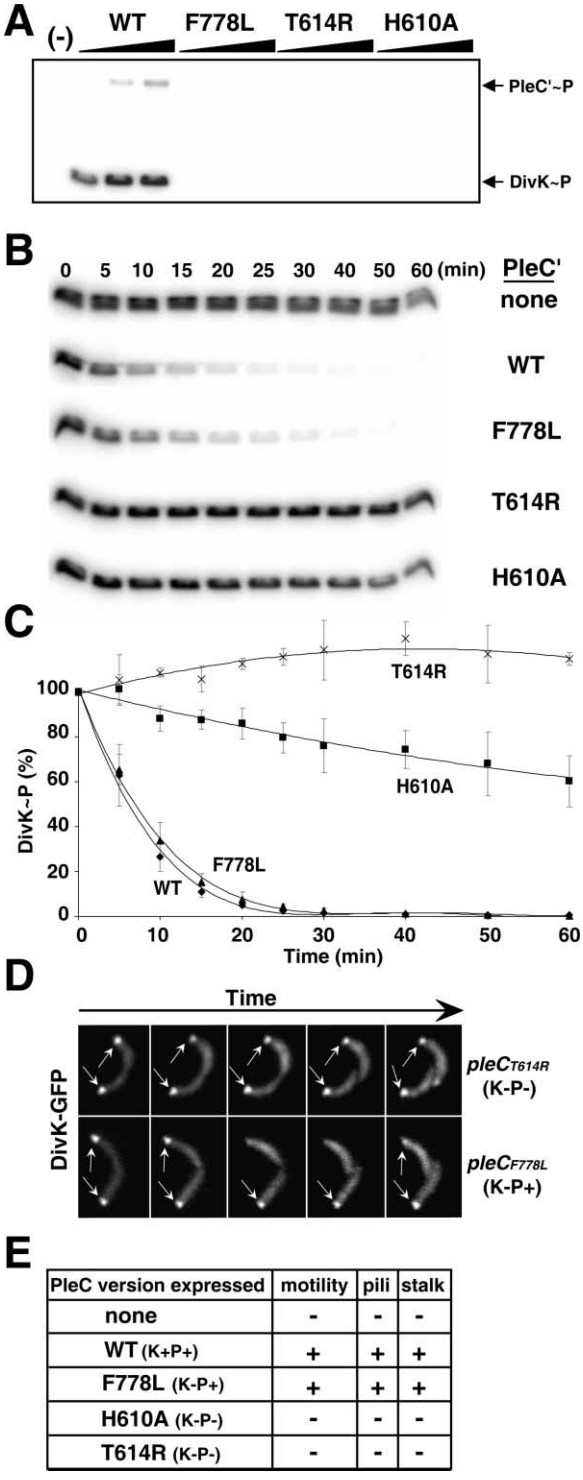

E

PleC version expressed	motility	pili	stalk
none	-	-	-
WT (K+P+)	+	+	+
F778L (K-P+)	+	+	+
H610A (K-P-)	-	-	-
T614R (K-P-)	-	-	-

Figure 3. PleC Predominantly Acts as a Phosphatase of DivK-P to Control SwaPS Development

(A) Kinase assay. DivK (0.5 μM) and γ^{32}-ATP were incubated in the reaction buffer alone (−) or with increasing concentrations of PleC′ and PleC′ mutant proteins (0.2, 0.5, and 1 μM) for 20 min. Autokinase activity (PleC′-P) and phosphotransfer to DivK (DivK-P) were visualized by phosphoimaging.

(B) Phosphatase assay. Time course of dephosphorylation of purified DivK-P (0.5 μM) in the absence or presence of PleC′ proteins (0.2 μM). Samples were transferred at the indicated times to SDS buffer and subjected to electrophoresis followed by phosphoimaging.

(C) Photodensitometry of DivK-P decay in the presence of PleC′ proteins after normalization for DivK autophosphatase activity.

(D) Time-lapse experiment of DivK-GFP localization in *pleC*::Tn*5* strain expressing K^-P^- $PleC_{T614R}$ (CJW1164) or K^-P^+ $PleC_{F778L}$ (CJW1162).

(E) K^-P^+ and K^-P^- PleC mutants were tested for their ability to complement the nonmotile, stalkless, and pililess phenotypes of a Δ*pleC* mutation. Motility and pili presence were examined using swarm agar and φCbK phage resistance assays (Sommer and Newton, 1991; Wang et al., 1993); φCbK phages use pili as receptors. Stalks were visualized by DIC microscopy.

erably reduced for $PleC'_{H610A}$. Strikingly, the $PleC'_{F778L}$ mutant displayed similar phosphatase activity to wild-type PleC′. Comparison of PleC′ mutants' phosphatase activity with that of wild-type PleC′ after normalization of DivK-P autophosphatase activity is shown in Figure 3C. Thus, while the T614R and H610A mutations generated kinase- and phosphatase-defective (K^-P^-) mutants, the F778L mutation successfully uncoupled the phosphatase activity of PleC from its kinase activity by creating a kinase-defective, phosphatase-active (K^-P^+) mutant.

If the phosphatase activity of PleC rather than its kinase activity fulfills the cytokinesis-dependent release of DivK from the flagellar pole to regulate SwaPS development in vivo, the K^-P^+ $PleC_{F778L}$ mutant but not the K^-P^- $PleC_{T614R}$ and $PleC_{H610A}$ mutants should be able to perform PleC developmental functions. Consistent with this hypothesis, time-lapse experiments of *pleC*::Tn*5* cells expressing the different PleC mutants revealed that, despite its lack of kinase activity, K^-P^+ $PleC_{F778L}$ successfully promoted DivK-GFP release from the flagellar pole upon cytokinesis (Figure 3D). In contrast, K^-P^- $PleC_{T614R}$ and $PleC_{H610A}$ failed to mediate DivK-GFP release at cell division (Figure 3D; Lam et al., 2003). Furthermore, the K^-P^+ $PleC_{F778L}$ mutant but not the K^-P^- $PleC_{T614R}$ and $PleC_{H610A}$ mutants were able to complement the pililess, stalkless, and nonmotile defects of a Δ*pleC* mutant (summarized in Figure 3E). The $pleC_{H610A}$ phenotypes had been previously described (Lam et al., 2003; Viollier et al., 2002); we show here that they can be attributed to the lack of PleC phosphatase activity. Thus, PleC is primarily a phosphatase of DivK-P in vivo, and this phosphatase activity promotes DivK release from the flagellar pole to initiate the SwaPS developmental program upon completion of cytokinesis.

Early Colocalization of DivJ and PleC with DivK at Opposite Poles during the Cell Cycle

Given the role of DivJ and PleC in the regulation of DivK localization at the flagellar pole, it was important to obtain an accurate temporal sequence of the subcellular distribution of PleC, DivJ, and DivK relative to each other during the cell cycle. To do this, the localization of all three proteins (each labeled with a different fluorophore) was examined in the same cells. We used two different strains to vary the combination of fluorophore tags. In the first one (CJW799), *divK*, *pleC*, and *divJ* were fused to *mcfp*, *myfp*, and *tdimer2* (a derivative of the *Discosoma* coral *dsRed* present in tandem), respectively. In the sec-

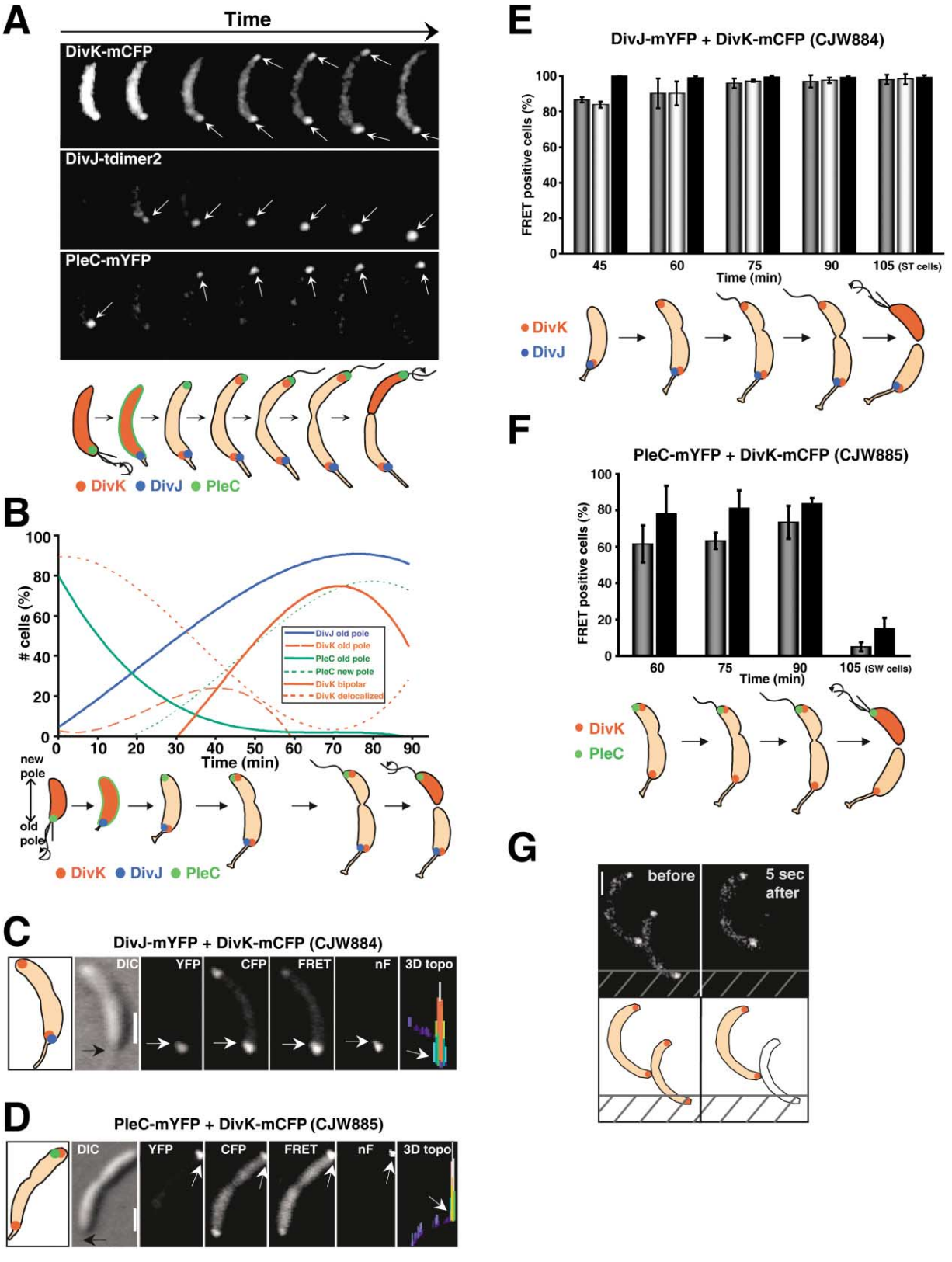

Figure 4. DivJ and PleC Promote Dynamic Polar Localization of DivK with Rapid Exchange of DivK between Polar Pools throughout the Predivisional Stage Preceding Completion of Cytokinesis

(A) Time-lapse fluorescence microscopy experiment starting with a synchronized swarmer cell population of strain CJW977 coexpressing DivK-mCFP, DivJ-tdimer2, and PleC-mYFP. White arrows show the polar signals. Below is a schematic of the subcellular distribution of all three fluorescently labeled proteins during the cell cycle.

ond strain (CJW801), *divK*, *pleC*, and *divJ* were fused to *mcfp*, *tdimer2*, and *yfp*, respectively. Both strains exhibited wild-type development and cell cycle. Similarly to the GFP, CFP, or YFP derivatives (Jacobs et al., 2001; Lam et al., 2003; Viollier et al., 2002; Wheeler and Shapiro, 1999), fusions of DivK, DivJ, and PleC to mCFP, mYFP, or tdimer2 supported the known wild-type functions of the untagged protein when expressed as the only source of the protein (data not shown). All fluorescently labeled proteins also displayed a temporal and spatial pattern of localization consistent with previous observations obtained with single GFP fusions (Jacobs et al., 2001; Wheeler and Shapiro, 1999). A representative time-lapse experiment using strain CJW977 is shown in Figure 4A. Figure 4B depicts the results from time course experiments on synchronized cell populations of strain CJW801. The sequence of protein localization during the cell cycle was confirmed in short time-lapse experiments (data not shown). From these experiments, four important observations were made. First, DivJ localization at the nascent stalked pole after the swarmer-to-stalked cell transition preceded the accumulation of DivK at the same pole, consistent with the notion that DivJ recruits DivK to the stalked pole (Lam et al., 2003). Second, PleC formed a focus at the nascent flagellar pole in the early predivisional stage. Shortly after, DivK adopted a bipolar localization. From this point, DivK colocalized with DivJ and PleC at the respective stalked and flagellar pole for most of the predivisional stage. Upon cytokinesis, DivK was released from the PleC flagellar pole. Thus, PleC colocalized with DivK at the flagellar pole for an extended period of time ($\sim$30 min under our time course conditions) before completion of cytokinesis and DivK release from the flagellar pole.

Visualization of DivJ/DivK and PleC/DivK Interactions at the Poles using FRET Microscopy

The considerable lag between PleC/DivK colocalization at the flagellar pole and the observed PleC-mediated release of DivK from that pole led us to question whether or not PleC phosphatase activity was dependent on cytokinesis. Colocalization of two proteins at the resolution of light microscopy does not necessarily mean that they do in fact physically interact. To demonstrate protein-protein interaction requires spatial resolution that exceeds the optical limit of conventional epifluorescence microscopy. Therefore, we sought to develop a fluorescence resonance energy transfer (FRET) microscopy assay in our bacterial system to monitor the interaction of DivK with PleC in live cells at single cell resolution. Because DivJ kinase activity mediates DivK localization at the flagellar pole, we also examined DivJ/DivK interactions during the cell cycle. To visualize DivJ/DivK and PleC/DivK interactions by FRET microscopy, we constructed FRET strains coexpressing either DivK-mCFP and DivJ-mYFP or DivK-mCFP and PleC-mYFP. Monomeric variants of CFP and YFP were used to avoid an artifactual dimerization between CFP and YFP (Zacharias et al., 2002). FRET was detected using a three filter microscope procedure. Here, the FRET signal or net FRET (nF), which is reflective of DivJ-mYFP/DivK-mCFP or PleC-mYFP/DivK-mCFP interaction, was calculated by correcting the signal intensity in the FRET channel from the contaminating CFP bleed through and YFP direct activation that are inherent to the technique (see Experimental Procedures). As shown for strain CJW884, in which DivJ-mYFP and DivK-mCFP were coexpressed, nF was clearly detected at the stalked pole where DivJ-mYFP and DivK-mCFP colocalized (Figure 4C). No detectable nF signal was present at the opposite pole where DivK-mCFP was also present. This indicated that the CFP bleed through had been efficiently subtracted from the measurements and that the FRET signal was specific to an interaction between DivK and DivJ at the stalked pole. FRET at the stalked pole could also be visualized in a 3D topographical representation of nF values across the image (Figure 4C). Conversely, a significant nF signal was only observed at the flagellar pole where DivK-mCFP and PleC-mYFP colocalized in FRET strain CJW885 (Figure 4D). Thus,

(B) The relative cell cycle and pole-specific localization of PleC-tdimer2, DivJ-YFP, and DivK-mCFP were determined in a series of time course experiments starting with synchronized populations of swarmer CJW801 cells. A cell pole was denoted "new pole" if it originated from the last cell division or "old pole" otherwise. The percentage of cells with a specific localization was plotted as a function of time after synchrony (t = 0 min, n = 336; t = 10 min, n = 214; t = 20 min, n = 565; t = 30 min, n = 343; t = 40 min, n = 237; t = 50 min, n = 348; t = 60 min, n = 353; t = 75 min, n = 396; t = 90 min, n = 384); the SD was, on average, 5%. The graph is represented as polynomial trendlines (order 3). Below is a schematic of the cell cycle-dependent localization pattern of PleC, DivJ, and DivK.

(C and D) Visualization of DivJ/DivK and PleC/DivK interactions at single cell resolution by FRET microscopy. The net FRET (nF) indicative of DivJ-mYFP/DivK-mCFP (C) or PleC-mYFP/DivK-mCFP (D) interactions at the stalked or flagellar pole were visualized as a polar fluorescent signal or as a 3D topographical representation using strains coexpressing DivJ-mYFP and DivK-mCFP (CJW884) (C) or PleC-mYFP and DivK-mCFP (CJW885) (D). Black and white arrows show the stalk and polar fluorescent signals of interest, respectively. Scale bar, 1 μm.

(E) DivJ and DivK interact at the stalked pole throughout the time of colocalization. The percentage of FRET-positive cells from synchronized cell populations of strain CJW884 coexpressing DivJ-mYFP and DivK-mCFP was determined every 15 min, starting with the 45 min time point after synchrony, which corresponded to the time of DivJ-mYFP and DivK-mCFP colocalization at the stalked pole (t = 45 min, n = 149; t = 60 min; n = 235; t = 75 min; n = 241; t = 90 min; n = 276; t = 105 min, n = 225). Cells were considered FRET-positive based upon statistical analysis using three different filtering methods (method 1, dark gray; method 2, light gray; and method 3, black; see Supplemental Data).

(F) PleC and DivK interact at the flagellar pole throughout the time of colocalization. The percentage of FRET-positive cells from synchronized cell populations of strain CJW885 coexpressing PleC-mYFP and DivK-mCFP was determined every 15 min, starting with the 60 min time point after synchrony, which corresponds to the time of PleC-mYFP and DivK-mCFP colocalization at the nascent flagellar pole (t = 60 min, n = 109; t = 75 min, n = 213; t = 90 min, n = 221; t = 105 min, n = 276). After FRET measurements, the cells were subjected to statistical analysis using filtering methods 1 (dark gray) and 3 (black).

(G) Polar localization of DivK is highly dynamic, with rapid exchange of DivK molecules between cytoplasmic and polar pools. Photobleaching experiment performed on predivisional cells (CJW366) expressing DivK-GFP. Images were taken before and after selectively photobleaching for 3–4 s an area (hatched bars) encompassing one pole of a cell with a laser. Scale bar, 1 μm.

our FRET microscopy method successfully detects the physical interaction of DivJ and PleC with DivK at the poles where colocalization occurs.

The Timing of DivJ and PleC Interaction with DivK at Opposite Poles Corresponds to the Timing of Their Colocalization

Using this FRET technique, we monitored DivJ and PleC interaction with DivK during the cell cycle. Under our experimental time course conditions, DivJ-mYFP and DivK-mCFP colocalized at the nascent stalked pole about 45 min after synchronization of swarmer cell populations. At each following 15 min time point, we quantified the number of cells with a statistically significant FRET signal (FRET-positive cells) at the stalked pole based on three different filtering methods (see Supplemental Data at http://www.cell.com/cgi/content/full/118/5/579/DC1 for a description of the statistical analyses). As shown in Figure 4E for strain CJW884, the percentage of FRET-positive cells was high at the 45 min time point using all three filtering methods, indicating that DivJ-mYFP interacted with DivK-mCFP at the stalked pole upon colocalization. The percentage of FRET-positive cells remained statistically similar for later time points, indicating that DivJ-mYFP and DivK-mCFP sustained their interaction at the stalked pole throughout the remainder of the cell cycle.

To define the temporal pattern of PleC-mYFP/DivK-mCFP interaction at the flagellar pole during the cell cycle, we performed FRET measurements on synchronized cell populations of strain CJW885. In this strain, FRET between DivK-mCFP and PleC-mYFP often resulted in quenching of the CFP emission signal in the CFP channel (I_{CFP}). This quenching resulted in I_{CFP} values approaching or equaling zero. Therefore, filtering method 2, which was based on nF/I_{CFP} ratios (see Supplemental Data on the *Cell* web site), could not be used to determine the number of FRET-positive cells. Nevertheless, both filtering methods 1 and 3 showed that most cells exhibited a significant FRET signal at the first time point of colocalization ($t = 60$ min; Figure 4F), indicating that PleC-mYFP and DivK-mCFP interacted at the nascent flagellar pole as soon as these two proteins colocalized. This interaction was maintained throughout the time of polar colocalization of these two proteins (75 and 90 min time points). The percentage of FRET-positive cells dramatically dropped at 105 min, corresponding to the release of DivK-mCFP from the flagellar pole after cytokinesis.

In conclusion, these FRET experiments indicate that DivJ and PleC interact with DivK upon colocalization at their respective poles and continue to interact with DivK throughout the time of polar colocalization during the cell cycle.

Rapid Exchange of DivK Molecules between Flagellar and Stalked Polar Pools

The temporal pattern of DivJ/DivK and PleC/DivK interactions suggests a model in which the localization of DivK at the flagellar pole results from the balancing activities of PleC phosphatase and DivJ kinase at opposite poles throughout the predivisional stage prior to completion of cytokinesis. In this model, PleC-mediated release of DivK from the flagellar pole is immediately compensated for by DivJ-induced localization of DivK-P to the flagellar pole. Because PleC and DivJ are located at opposite poles, this model implies a highly dynamic polar localization of DivK with a rapid exchange of DivK molecules between polar pools through diffusion in the cytoplasm. Cytoplasmic diffusion is thought to be very rapid in bacteria; the diffusion coefficient for GFP in *E. coli* is $\sim$8 $\mu m^2/s$ (Elowitz et al., 1999). To test this model, we examined the dynamism of DivK polar localization in fluorescence photobleaching experiments. Predivisional cells with bipolar DivK-GFP were imaged before and after photobleaching an area encompassing a cell pole until complete extinction of the polar signal ($\sim$4 s). During this short time interval, loss of fluorescence at one pole was always accompanied by the disappearance of fluorescence from the cytoplasm and distal pole (Figure 4G). Thus, within seconds, all DivK-GFP molecules in the cell (including those that were once in the cytoplasm and at the distal pole) had passed through the photobleached pole, indicating a rapid exchange of DivK-GFP between cytoplasmic and polar pools of the protein. The accuracy of the laser beam was attested by the absence of photobleaching in neighboring cells located outside the bleached zone (Figure 4G). The results were similar, regardless of the nature of the pole (stalked or flagellar). Thus, DivK does not remain anchored to the poles during the predivisional phase when bipolar foci of DivK are observed ($\sim$30 min). Instead, bipolar localization of DivK is a very dynamic process, in which DivK molecules from the flagellar and stalked polar pools are continuously exchanged within seconds or less through cytoplasmic diffusion and localized actions of DivJ kinase and PleC phosphatase at opposite poles.

Cytokinesis Interrupts the Rapid Exchange of DivK Molecules between Polar Pools

As shown in Figure 2B, failure to execute cytokinesis resulted in filamentous cells unable to completely release DivK from the flagellar pole, thereby blocking entry into SwaPS development. FRET microscopy on FtsZ-depleted strains coexpressing DivJ-mYFP and DivK-mCFP (CJW979) or PleC-mYFP and DivK-mCFP (CJW981) indicated that DivJ/DivK and PleC/DivK interactions at opposite poles were maintained throughout cell filamentation; all three FRET filtering methods showed a constant percentage of FRET-positive cells over time when cytokinesis was inhibited (Figure 5A). We also performed photobleaching experiments with FtsZ-depleted filamentous cells expressing bipolar DivK-GFP. In these filamentous cells (unlike normal-sized cells, Figure 4G), it was technically possible to photobleach one cell pole without photobleaching the rest of the cell (Figure 5B). Fluorescence recovery of DivK-GFP fluorescence at the photobleached pole was observed 5 s later, indicating that the rapid exchange of DivK-GFP between polar and cytoplasmic pools was maintained in these filamentous cells (Figure 5B). These fluorescence recovery after photobleaching (FRAP) experiments were possible with filamentous cells and not with normal sized cells, presumably because the greater distance between poles sufficiently slowed down the dynamic exchange of DivK between polar pools.

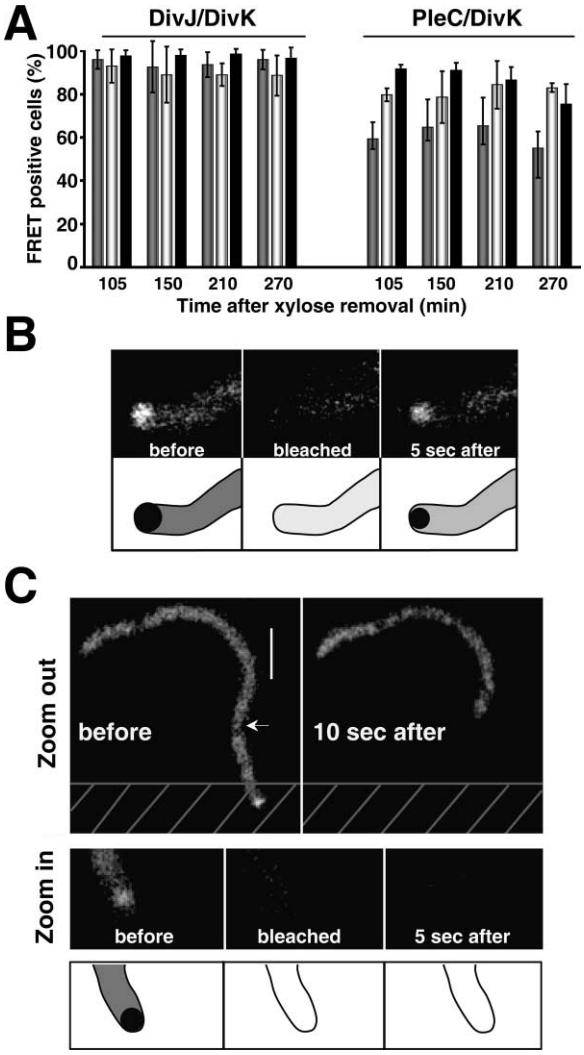

Figure 5. Inhibition of Cytokinesis Sustains PleC/DivK and DivJ/DivK Polar Interactions, which, in Turn, Results in Dynamic Polar Localization of DivK with Rapid Exchange of DivK between Polar Pools

(A) The percentage of FRET-positive cells indicative of interactions between DivJ-mYFP and DivK-mCFP (strain CJW979) or between PleC-mYFP and DivK-mCFP (strain CJW981) remained constant after FtsZ depletion. Cells were considered FRET-positive upon statistical analysis using three filtering methods (method 1, dark gray; method 2, light gray; and method 3, black; see Supplemental Data). For CJW979 cells, t = 105 min, n = 209; t = 150 min, n = 141; t = 210 min, n = 116; t = 270 min, n = 152. For CJW981 cells, t = 105 min, n = 164; t = 150 min, n = 130; t = 210 min, n = 118; t = 270 min, n = 91.

(B) FRAP experiment was performed on elongated FtsZ-depleted cells (CJW933). DivK-GFP was selectively photobleached at one pole for 3–4 s, and recovery of the polar fluorescence signal was observed 5 s later.

(C) Photobleaching of one pole of an elongated CJW933 cell in which cytokinesis had been restored by addition of xylose resulted in a complete loss of polar and cytoplasmic DivK-GFP fluorescence up to the site of cell division (arrow), with no fluorescence recovery at the bleached pole. Hatched bars shows the bleached area. Scale bar, 1 μm.

As mentioned above, restoration of cytokinesis by addition of xylose to cultures of filamentous cells resulted in DivK release from the flagellar pole (as illustrated in Figure 2C). As expected, photobleaching experiments showed that restoration of cytokinesis in elongated cells prevented fluorescence recovery at the photobleached pole, indicative of an inhibition of DivK-GFP shuttling between the two poles (Figure 5C; arrow shows site of cytokinesis).

Thus, these experiments on filamentous cells indicate that the cell does not measure time or cell length to regulate DivK localization at the flagellar pole. Rather, the dynamism of DivK polar localization, which primarily relies on localized activities of DivJ and PleC at opposite poles, suggests that the cell monitors the cytoplasmic communication between the poles.

A Ping-Pong Mechanism that Monitors Cytokinesis to Control Initiation of SwaPS Development

Taken together, our data suggest that the dynamic polar localization of DivK participates in a mechanism that monitors cytokinesis to regulate SwaPS development (Figure 6). In the predivisional stage when the cell is a single cytoplasmic unit, PleC phosphatase and compensating DivJ kinase activities localized at opposite poles, together with fast cytoplasmic diffusion, mediate dynamic polar localization of DivK with a rapid "Ping-Pong" exchange of DivK and DivK-P molecules between poles. This dynamic process maintains a steady-state localization of DivK-P at the flagellar pole, which, in turn, inhibits SwaPS development. Completion of cytokinesis creates a cytoplasmic diffusion barrier, which effectively segregates DivJ and PleC activities and interrupts the rapid DivK/DivK-P exchange between the DivJ stalked pole and the PleC flagellar pole. The PleC phosphatase-mediated release of DivK from the flagellar pole is therefore no longer compensated for by DivJ kinase-induced localization of DivK-P. This results in a complete release of DivK from the flagellar pole, allowing the initiation of SwaPS development. This Ping-Pong mechanism thereby couples SwaPS development to completion of cytokinesis during normal cell cycle progression. In addition, this proposed mechanism appears to participate in a checkpoint control that blocks SwaPS development when cytokinesis fails. Absence or incomplete cytokinesis results in the maintenance of the Ping-Pong exchange of DivK and DivK-P between poles, thereby preventing initiation of SwaPS development. Resumption of cytokinesis in cell filaments disrupts the DivK/DivK-P shuttling between poles and triggers development of the swarmer progeny.

How is the development of the stalked progeny regulated? Interestingly, morphogenesis of the stalked cell, which includes the assembly of a flagellum at the pole opposite the stalk, is not dependent on previous cytokinesis; instead, it depends on DNA replication (Osley and Newton, 1977; Osley et al., 1977). This may be because stalked cells can originate not only from asymmetric divisions but also from the differentiation of swarmer cells (Figure 1), rendering a cytokinesis-dependent mechanism inappropriate. A dependency on DNA replication would provide a common control mechanism for stalked cells of both origins, because DNA replication begins in the stalked cell immediately after division and is prevented in the swarmer cell until it has developed into a stalked cell. The nature of the control mechanism

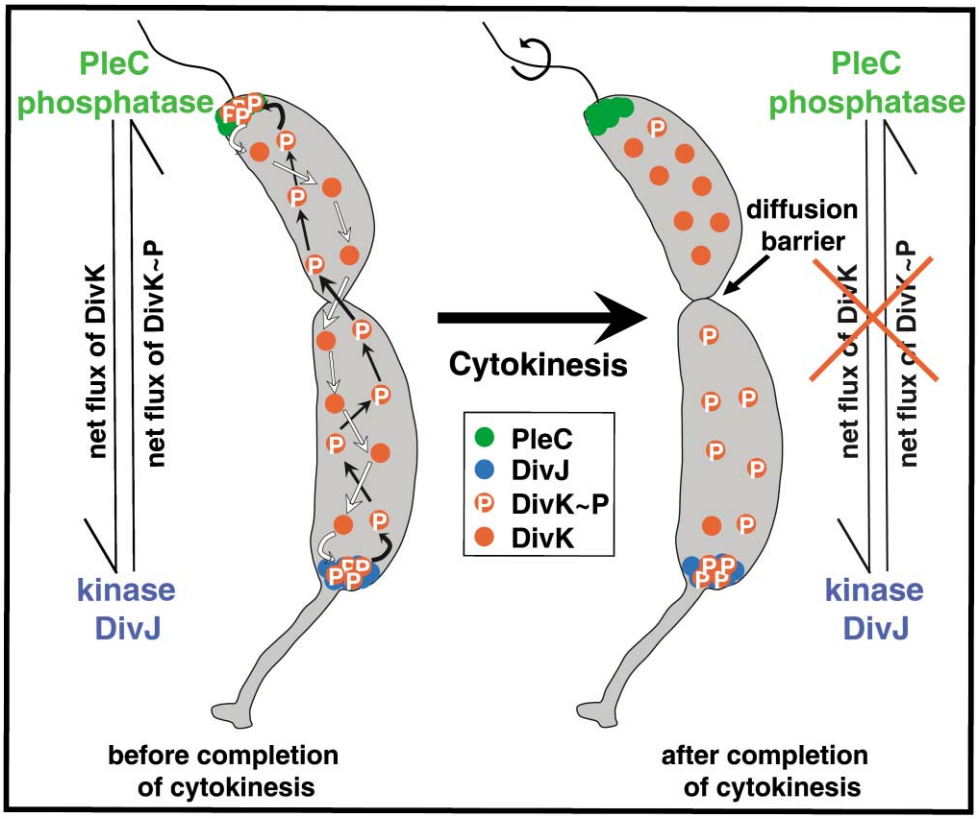

Figure 6. Model Depicting How the Cell Monitors Cytokinesis to Control SwaPS Development

In the predivisional cell in which the cytoplasm is continuous between cell poles, PleC phosphatase promotes the release of DivK from the (DivK-P high-affinity) flagellar pole by dephosphorylating DivK-P. However, this DivK release is immediately counteracted by DivJ kinase activity, which, by phosphorylating DivK, mediates compensatory DivK-P localization to the flagellar pole. Because DivJ and PleC are located at opposite poles, their compensating activities on DivK phosphorylation and localization result in a dynamic localization of DivK at the pole with rapid exchange of DivK-P and DivK between poles through fast diffusion in the cytoplasm. As long as there is a cytoplasmic communication between the PleC flagellar and DivJ stalked poles, accumulation of DivK-P at the flagellar pole is maintained, thereby preventing premature SwaPS development. Upon completion of cytokinesis, segregation of PleC and DivJ into two different daughter cells disrupts the DivK/DivK-P cytoplasmic exchange between PleC and DivJ poles. The PleC phosphatase-mediated release of DivK from the flagellar pole is no longer compensated for by DivJ kinase activity, resulting in complete cytoplasmic dispersion of DivK from the flagellar pole and hence induction of SwaPS development.

is unknown. Intriguingly, the $DivK_{D90G}$ mutant exhibits a cold sensitive phenotype at 24°C where it is unable to localize to not only the flagellar pole but also the stalked pole (H.L., unpublished data). This defect at 24°C is accompanied by inhibition of DNA replication (Hung and Shapiro, 2002), suggesting a possible link between DivK localization at the stalked pole and DNA replication.

How could the subcellular localization of DivK affect development? Genetic evidence with the localization mutant *divK*$_{D90G}$ has linked DivK to the degradation of the swarmer cell fate determinant CtrA in stalked cells upon cytokinesis or swarmer cell differentiation (Hung and Shapiro, 2002; Wu et al., 1998). CtrA directly controls the transcription of about 100 cell cycle-regulated genes, many of which are involved in development (Laub et al., 2002). It is also possible that DivK affects the activity of more than one downstream effector. For instance, Δ*pleD* mutants fail to shed their flagella and are mostly defective in stalk formation (Aldridge and Jenal, 1999; Sommer and Newton, 1989). DivK may therefore control flagellum shedding and stalk formation through the PleD response regulator whose gene is organized in an operon with *divK*. Furthermore, it was recently shown that phosphorylation and localization of PleD at the stalked pole regulates PleD's diguanylate cyclase activity in a DivJ- and PleC-dependent manner (Paul et al., 2004).

In any case, this study identifies a mechanism that uses polar localization of signaling proteins to ultimately control developmental events in response to completion of cytokinesis. From *Bacillus subtilis* sporulation to larval development in nematodes to neurogenesis in flies and mammals, developmental decisions are often intimately coupled with asymmetric cell divisions (Doe and Bowerman, 2001; Knoblich, 2001; Losick and Dworkin, 1999; Lu et al., 2000). The polar localization of proteins has been recognized as an important mechanism governing cell differentiation in many organisms. For example, the process of neural differentiation in *Drosophila* relies on the cell cycle-dependent localization of proteins at opposite poles of the mother cell, which ultimately dictates the differentiation and fate of the progeny (Doe and

Bowerman, 2001; Knoblich, 2001). Premature cell differentiation in the mother cell would probably be deleterious to cell type diversity and development of the organism. Therefore, control mechanisms, perhaps similar to the one described here, may operate in higher organisms to ensure that cell differentiation does not occur before completion of cell division.

Experimental Procedures

Strains, Plasmids, and Media

Caulobacter strains were grown at 30°C (unless otherwise stated) in PYE (peptone yeast extract), M5GG, or M2G supplemented with 1% PYE (Lam et al., 2003). Plasmids were mobilized from *E. coli* strain S17-1 into *Caulobacter* by bacterial conjugation (Ely, 1991). Plasmids and strains are listed in Table 1, and the strategies for their construction are available upon request. When needed, homogenous swarmer cell populations were obtained as described (Evinger and Agabian, 1977).

Protein Purification and In Vitro Phosphorylation Assays

Sequences encoding the catalytic domain of PleC (PleC′) and full-length DivK were cloned in a pET28c expression vector (Novagen, WI), and expression was induced with 1 mM IPTG for 4 hr at 37°C. The resulting His fusions were affinity purified with a Co^{2+} chelated resin (BD TALON resin, BD Biosciences, CA). Untagged DivK was obtained by cleaving His-DivK with Thrombin (Novagen, WI) for 16 hr at 20°C, followed by purification by ion exchange chromatography. Kinase and phosphatase assays were carried out as described (Hecht et al., 1995) with the following modification for the purification of DivK-P: two rounds of in-batch purification with the TALON resin were performed after gel filtration of the kinase reaction to purify DivK-P from any contaminating His-tagged PleC′.

Microscopy and Photography

Cells were placed on a slide that was layered with a 1% agarose pad containing M2G (Jacobs et al., 2001). Fluorescence and FRET microscopy was performed using a Nikon E1000 microscope equipped with a 100× DIC objective and appropriate filter sets (Chroma Technology Corp., VT). Images were taken with a Hamamatsu Orca-ER LCD camera, except for the cell cycle time-lapse experiments with strain CJW977, for which a Roper Photometrics Cascade 512:B camera was used. Images were analyzed with Metamorph software (Universal Imaging, PA). For the photobleaching experiments, we used a Bio-Rad MRC-1024 Laser Scanning Imaging System attached to a Zeiss Axiovert 35 microscope equipped with a Zeiss 100× Plan Apo objective and a Krypton/Argon mixed gas laser. Fluorescence photobleaching was obtained by iterative illumination at 488 nm. Electron microscopy was performed as described (Osley and Newton, 1977).

FRET Measurements

FRET strains coexpressed either DivK-mCFP and DivJ-mYFP or DivK-mCFP and PleC-mYFP. Each FRET strain had a corresponding set of control strains in which each of the fusion proteins was expressed separately. In some of these strains, the fusions were plasmid encoded to improve the signal intensities, which was important to obtain statistically significant FRET measurements. This protein overexpression did not affect the cell cycle mechanism of PleC-mediated release of DivK. The temporal and spatial PleC/DivK and DivJ/DivK colocalization, the PleC-mediated release of DivK, and the activation of morphogenesis in response to the completion of cytokinesis were accurately recapitulated in all FRET strains. A significant FRET signal between DivJ-mYFP and DivK-mCFP or between PleC-mYFP and DivK-mCFP was also observed at the stalked or flagellar pole using strains CJW865 or CJW718, in which *divJ-myfp* or *pleC-myfp* was chromosomally expressed, respectively (data not shown); however, the weakness of the signals resulted in greater variability in net FRET (nF) values between cells and a decreased sensitivity, rendering these strains less suited for FRET measurements.

For FRET measurements, images were acquired in the order of DIC, FRET, CFP, and YFP using appropriate filter sets and exposure times of 75 ms, 500 ms, 500 ms, and 1200 ms, respectively. Because polar protein signals were only ~15 pixels covering a nongeometrical area, it was not possible to determine the average intensity of the entire area without including pixels from the background or from the rest of the cell. Thus, by convention, we measured the brightest pixel intensity (I_{max}) within a square region drawn around the cell pole using Metamorph software. The net signal intensity (I) was determined by subtracting the cytoplasmic background intensity (I_{av}; average intensity along a line drawn into the cell) from I_{max}. This was done for each channel using the same regions of interest. The real FRET signal (nF) in FRET strains was obtained by applying the conventional equation: $nF = I_{FRET} - (I_{CFP} \times b) - (I_{YFP} \times a)$, where b is a norm of the percentage of CFP bleed through, and a is a norm of the percentage of direct excitation of YFP in the FRET channel (Xia and Liu, 2001; Youvan et al., 1997). The norms a and b were determined using cells expressing only mCFP or mYFP (control strains) and quantifying I_{FRET}/I_{CFP} or I_{FRET}/I_{YFP} ratios. The averaged b value was 0.36, indicating that 36% of the CFP signal contaminated the FRET signal; this was similar, regardless of the nature of the pole or the cell cycle stage. The averaged a values were minimal and ranged between 0.06 and 0.09, depending on the control strain, meaning that 6%–9% of the FRET signal resulted from a direct excitation of mYFP by CFP excitation wavelengths. Three different statistical methods were used to determine the number of FRET-positive cells (see Supplemental Data).

Acknowledgments

We thank Frank Slack, Nora Ausmees, and the members of the Jacobs-Wagner laboratory for critical reading of the manuscript. We are also grateful to Shannon Renn for generating the *pleC*$_{T614R}$ mutant. We also thank Tom Pollard's laboratory for their help with protein purification and R.Y. Tsien for constructs carrying *mcfp*, *myfp*, and *tdimer2*. This work was supported by National Institutes of Health grant GM065835 (C.J.-W.); the Pew Scholars Program in the Biological Sciences, sponsored by the Pew Charitable Trusts (C.J.-W.); and fellowships from the Belgian American Educational Foundation (New Haven, CT), Télévie (Brussels, Belgium), and the Foundation Léon Frédéricq (Liège, Belgium) (J.-Y.M.).

Received: May 11, 2004
Revised: July 16, 2004
Accepted: July 21, 2004
Published: September 2, 2004

References

Aiba, H., Nakasai, F., Mizushima, S., and Mizuno, T. (1989). Evidence for the physiological importance of the phosphotransfer between the two regulatory components, EnvZ and OmpR, in osmoregulation in *Escherichia coli*. J. Biol. Chem. *264*, 14090–14094.

Aldridge, P., and Jenal, U. (1999). Cell cycle-dependent degradation of a flagellar motor component requires a novel-type response regulator. Mol. Microbiol. *32*, 379–391.

Alley, M.R. (2001). The highly conserved domain of the *Caulobacter* McpA chemoreceptor is required for its polar localization. Mol. Microbiol. *40*, 1335–1343.

Campbell, R.E., Tour, O., Palmer, A.E., Steinbach, P.A., Baird, G.S., Zacharias, D.A., and Tsien, R.Y. (2002). A monomeric red fluorescent protein. Proc. Natl. Acad. Sci. USA *99*, 7877–7882.

Doe, C.Q., and Bowerman, B. (2001). Asymmetric cell division: fly neuroblast meets worm zygote. Curr. Opin. Cell Biol. *13*, 68–75.

Elowitz, M.B., Surette, M.G., Wolf, P.E., Stock, J.B., and Leibler, S. (1999). Protein mobility in the cytoplasm of *Escherichia coli*. J. Bacteriol. *181*, 197–203.

Ely, B. (1991). Genetics of *Caulobacter crescentus*. Methods Enzymol. *204*, 372–384.

Evinger, M., and Agabian, N. (1977). Envelope-associated nucleoid from *Caulobacter crescentus* stalked and swarmer cells. J. Bacteriol. *132*, 294–301.

Hecht, G.B., Lane, T., Ohta, N., Sommer, J.M., and Newton, A. (1995). An essential single domain response regulator required for normal cell division and differentiation in *Caulobacter crescentus*. EMBO J. *14*, 3915–3924.

Hsing, W., and Silhavy, T.J. (1997). Function of conserved histidine-243 in phosphatase activity of EnvZ, the sensor for porin osmoregulation in *Escherichia coli*. J. Bacteriol. *179*, 3729–3735.

Hsing, W., Russo, F.D., Bernd, K.K., and Silhavy, T.J. (1998). Mutations that alter the kinase and phosphatase activities of the two-component sensor EnvZ. J. Bacteriol. *180*, 4538–4546.

Huguenel, E.D., and Newton, A. (1982). Localization of surface structures during procaryotic differentiation: role of cell division in *Caulobacter crescentus*. Differentiation *21*, 71–78.

Hung, D.Y., and Shapiro, L. (2002). A signal transduction protein cues proteolytic events critical to *Caulobacter* cell cycle progression. Proc. Natl. Acad. Sci. USA *99*, 13160–13165.

Jacobs, C., Hung, D., and Shapiro, L. (2001). Dynamic localization of a cytoplasmic signal transduction response regulator controls morphogenesis during the *Caulobacter* cell cycle. Proc. Natl. Acad. Sci. USA *98*, 4095–4100.

Knoblich, J.A. (2001). Asymmetric cell division during animal development. Nat. Rev. Mol. Cell Biol. *2*, 11–20.

Lam, H., Matroule, J.Y., and Jacobs-Wagner, C. (2003). The asymmetric spatial distribution of bacterial signal transduction proteins coordinates cell cycle events. Dev. Cell *5*, 149–159.

Laub, M.T., Chen, S.L., Shapiro, L., and McAdams, H.H. (2002). Genes directly controlled by CtrA, a master regulator of the *Caulobacter* cell cycle. Proc. Natl. Acad. Sci. USA *99*, 4632–4637.

Losick, R., and Dworkin, J. (1999). Linking asymmetric division to cell fate: teaching an old microbe new tricks. Genes Dev. *13*, 377–381.

Lu, B., Jan, L., and Jan, Y.N. (2000). Control of cell divisions in the nervous system: symmetry and asymmetry. Annu. Rev. Neurosci. *23*, 531–556.

Ohta, N., and Newton, A. (1996). Signal transduction in the cell cycle regulation of *Caulobacter* differentiation. Trends Microbiol. *4*, 326–332.

Ohta, N., and Newton, A. (2003). The core dimerization domains of histidine kinases contain recognition specificity for the cognate response regulator. J. Bacteriol. *185*, 4424–4431.

Ohta, N., Grebe, T.W., and Newton, A. (2000). Signal transduction and cell cycle checkpoints in developmental regulation of *Caulobacter*. In Prokaryotic Development, Y.V. Brun and L.J. Shimkets, eds. (Washington, D.C.: American Society for Microbiology), pp. 341–359.

Osley, M.A., and Newton, A. (1977). Mutational analysis of developmental control in *Caulobacter crescentus*. Proc. Natl. Acad. Sci. USA *74*, 124–128.

Osley, M.A., Sheffery, M., and Newton, A. (1977). Regulation of flagellin synthesis in the cell cycle of *Caulobacter*: dependence on DNA replication. Cell *12*, 393–400.

Paul, R., Weiser, S., Amiot, N.C., Chan, C., Schirmer, T., Giese, B., and Jenal, U. (2004). Cell cycle-dependent dynamic localization of a bacterial response regulator with a novel di-guanylate cyclase output domain. Genes Dev. *18*, 715–727.

Roberts, R.C., Toochinda, C., Avedissian, M., Baldini, R.L., Gomes, S.L., and Shapiro, L. (1996). Identification of a *Caulobacter crescentus* operon encoding *hrcA*, involved in negatively regulating heat-inducible transcription, and the chaperone gene *grpE*. J. Bacteriol. *178*, 1829–1841.

Simon, R., Prieffer, U., and Puhler, A. (1983). A broad host range mobilization system for *in vivo* genetic engineering: transposon mutagenesis in gram-negative bacteria. Biotechnology *1*, 784–790.

Sommer, J.M., and Newton, A. (1989). Turning off flagellum rotation requires the pleiotropic gene *pleD*: *pleA*, *pleC*, and *pleD* define two morphogenic pathways in *Caulobacter crescentus*. J. Bacteriol. *171*, 392–401.

Sommer, J.M., and Newton, A. (1991). Pseudoreversion analysis indicates a direct role of cell division genes in polar morphogenesis and differentiation in *Caulobacter crescentus*. Genetics *129*, 623–630.

Spratt, B.G., Hedge, P.J., te Heesen, S., Edelman, A., and Broome-Smith, J.K. (1986). Kanamycin-resistant vectors that are analogues of plasmids pUC8, pUC9, pEMBL8 and pEMBL9. Gene *41*, 337–342.

Terrana, B., and Newton, A. (1976). Requirement of a cell division step for stalk formation in *Caulobacter crescentus*. J. Bacteriol. *128*, 456–462.

Tomoromi, C., Kurokawa, H., and Ikura, M. (2003). The histidine kinase family: structures of essential building blocks. In Histidine Kinases in Signal Transduction, M. Inouye and R. Dutta, eds. (Amsterdam: Elsevier Science), pp. 11–24.

Viollier, P.H., Sternheim, N., and Shapiro, L. (2002). A dynamically localized histidine kinase controls the asymmetric distribution of polar pili proteins. EMBO J. *21*, 4420–4428.

Wang, S.P., Sharma, P.L., Schoenlein, P.V., and Ely, B. (1993). A histidine protein kinase is involved in polar organelle development in *Caulobacter crescentus*. Proc. Natl. Acad. Sci. USA *90*, 630–634.

Wang, Y., Jones, B.D., and Brun, Y.V. (2001). A set of *ftsZ* mutants blocked at different stages of cell division in *Caulobacter*. Mol. Microbiol. *40*, 347–360.

Wheeler, R.T., and Shapiro, L. (1999). Differential localization of two histidine kinases controlling bacterial cell differentiation. Mol. Cell *4*, 683–694.

Wu, J., Ohta, N., and Newton, A. (1998). An essential, multicomponent signal transduction pathway required for cell cycle regulation in *Caulobacter*. Proc. Natl. Acad. Sci. USA *95*, 1443–1448.

Xia, Z., and Liu, Y. (2001). Reliable and global measurement of fluorescence resonance energy transfer using fluorescence microscopes. Biophys. J. *81*, 2395–2402.

Youvan, D.C., Silva, C.M., Bylina, E.J., Coleman, M.R., Dilworth, M.R., and Yang, M.M. (1997). Calibration of fluorescence resonance energy transfer in microscopy using genetically engineered GFP derivatives on nickel chelating beads. Biotechnol. Alia *3*, 1–18.

Zacharias, D.A., Violin, J.D., Newton, A.C., and Tsien, R.Y. (2002). Partitioning of lipid-modified monomeric GFPs into membrane microdomains of live cells. Science *296*, 913–916.